Head and trunk in zebrafish arise via coinhibition of BMP signaling by *bozozok* and *chordino*

Encina M. Gonzalez,[1,3] Kimberly Fekany-Lee,[1,3]
Amanda Carmany-Rampey,[1] Caroline Erter,[2]
Jacek Topczewski,[1] Christopher V.E. Wright,[2]
and Lilianna Solnica-Krezel[1,4]

[1]Department of Biological Sciences, Vanderbilt University,
and [2]Department of Cell Biology, Vanderbilt University
School of Medicine, Nashville, Tennessee 37235, USA

Spatial variations in the levels of bone morphogenetic protein (BMP) signaling are a critical determinant of dorsoanterior-ventroposterior pattern in vertebrate embryos. Whereas BMP overexpression abolishes both head and trunk development, known single and double loss-of-function mutations in BMP inhibitors have less dramatic effects. We report that combining mutations in the zebrafish genes *bozozok* and *chordino* causes a synergistic loss of head and trunk, whereas most cells express ventro-posterior markers and develop into a tail. Genetic inactivation of BMP signaling fully suppresses these defects. Thus, a remarkably simple genetic mechanism, involving a coinhibition of BMP function by the partially overlapping *bozozok* and *chordino* pathways is used to specify vertebrate head and trunk.

During vertebrate development, secreted bone morphogenetic proteins 2/4/7 (BMPs) interact with extracellular antagonists produced by the dorsal (Spemann) gastrula organizer, such as Noggin and Chordin, establishing a ventral to dorsal gradient of BMP activity that specifies cell fates. In the gastrula, epidermis and blood are specified at highest BMP activity, somites are specified laterally, whereas axial mesoderm and neural tissue develop dorsally, at the levels of lowest BMP activity (Sasai et al. 1995; Wilson and Hemmati-Brivanlou 1995; Kishimoto et al. 1997; Nguyen et al. 1998; Nikaido et al. 1999). In frog and fish embryos, establishment of the gastrula organizer is initiated via maternally deposited factors that lead to nuclear accumulation of β-catenin dorsally (Schneider et al. 1996; Mizuno et al. 1999; Ober and Schulte-Merker 1999). At the onset of zygotic transcription, β-catenin activates expression of *nodal*-related

genes together with the homeobox genes *bozozok/dharma/nieuwkoid* (*bozozok*) in zebrafish, and *siamois*, *twin* in *Xenopus*; these genes cooperatively promote organizer formation (Brannon and Kimelmann 1996; Laurent et al. 1997; Fekany et al. 1999; Koos and Ho 1999; Shimizu et al. 2000; Sirotkin et al. 2000).

Ablation of dorsal determinants or other manipulations interfering with the nuclear localization of β-catenin, and surgical removal of the gastrula organizer, all cause progressive head-to-tail truncations (Scharf and Gerhart 1983; Jesuthasan and Strahle 1997; Mizuno et al. 1999; Ober and Schulte-Merker 1999). Such defects are phenocopied by ectopic BMP signaling in frog and fish embryos (Clement et al. 1995; Kishimoto et al. 1997; Neave et al. 1997), suggesting that inhibition of BMP signaling might be necessary for the specification of head, trunk, and tail tissues. However, various zebrafish and mouse mutations that diminish the ability of the gastrula organizer to limit BMP activity do not lead to a complete loss of head and trunk. The *chordino* (*din*) mutations (which inactivate the BMP antagonist Chordin), only mildly ventralize the zebrafish embryo, leading to excess blood and multiple finfolds, but normal AP pattern (Schulte-Merker et al. 1997). Moreover, simultaneous inactivation of *din* and *ogon* (*ogo*), encoding a molecularly uncharacterized negative regulator of BMP, while leading to a more ventralized phenotype than each of the single mutants, does not interfere with the formation of head, trunk, and tail (Miller-Bertoglio et al. 1999). Similarly, *chordin;noggin* double-mutant mice exhibit a loss of forebrain and axial mesoderm, but maintain a relatively well-formed anterior posterior (AP) axis (Bachiller et al. 2000). Mutations in the zebrafish homeobox gene *boz* lead to loss of forebrain, midbrain, and axial mesoderm due to an excess of both BMP and Wnt signaling (Koos and Ho 1999; Fekany-Lee et al. 2000). This phenotype is reminiscent of defects resulting from moderate levels of ectopic BMP activity (Kishimoto et al. 1997; Neave et al. 1997; Nguyen et al. 1998).

Inhibition of Nodal signaling by mutations in genes encoding Nodal-related ligands, Squint and Cyclops, also interferes with organizer formation and function, resulting in cyclopic embryos (Feldman et al. 1998; Rebagliati et al. 1998; Sampath et al. 1998). In *cyc;sqt* double mutants, severe deficiency of head and trunk mesoderm is observed, with apparent complete loss of anterior trunk spinal cord, but relatively normal brain AP pattern (Feldman et al. 1998). Simultaneous inactivation of *boz* and *squint* (*sqt*) or *cyclops* (*cyc*) genes leads to more severe organizer deficiencies and anterior truncations than in *boz* mutants alone, yet both *boz;sqt* and *boz;cyc* double mutants exhibit reduced head and trunk structures (Shimizu et al. 2000; Sirotkin et al. 2000). Even *boz;sqt;cyc* triple mutants develop a very reduced head featuring forebrain (Sirotkin et al. 2000). So far, although these studies suggest that multiple factors function redundantly to limit BMP activity in vivo, the number of early-acting genes involved remains unclear. The genetic

study presented here identifies the primary factors that are essential for limiting BMP signaling, and thereby provides insight into the early genetic hierarchy underlying head and trunk formation in vertebrate embryos.

Results and Discussion

To identify the key genes that cooperate in limiting BMP signaling during vertebrate axis formation, we have explored the functional interactions between *bozozok* (*boz*) and *chordino* (*din*) in zebrafish. Intriguingly, *boz* mutants exhibit reduced *din* expression, suggesting that these two genes act in partially overlapping pathways with respect to inhibition of BMP activity (Koos and Ho 1999; Fekany-Lee et al. 2000; Shimizu et al. 2000). To test how simultaneous elimination of *boz* and *din* affects BMP inhibition and axis formation, we constructed *boz din* double mutants. In crosses between boz^{m168+} din^{tt250+} fish (Schulte-Merker et al. 1997; Fekany et al. 1999), two phenotypic classes of *boz din* double mutants were observed, with variable frequency, at 1-day post fertilization (1 dpf). The less severely affected class exhibited a loss of notochord, severe head truncations, multiple fin folds, and an excess of blood cells near the anus (Fig. 1f,g). The more severely affected class displayed a complete loss of head and trunk structures, a protrusion at one end of the yolk cell, and a tail with ~10 somites and multiple fin folds (Fig. 1i, inset). The frequency of the strong class of *boz din* double mutants decreases with age of the female, as observed previously

for the *boz* mutant phenotype (Fekany et al. 1999). Among the double mutant progeny obtained from a mature female, the strong class constituted 39% (number of double mutants = 49; number of total progeny = 459). Results presented in our work describe the strong double-mutant phenotype. The combined incidence of both classes was lower than expected for independently segregating loci, consistent with *boz* and *din* being linked (Fekany et al. 1999). To facilitate further analysis, we utilized $boz^{m168/+}$ $din^{tt250/+}$ fish, in which recombination placed both mutations on the same chromosome.

To characterize the combined requirement for *boz* and *din* in head and trunk development, we analyzed the morphology of *boz din* mutants and expression of tissue-specific gene markers by whole-mount in situ hybridization (Thisse and Thisse 1998). In wild-type embryos, at the end of gastrulation (10 h post fertilization, hpf), cells had accumulated dorsally on the yolk forming an axis with a head rudiment at the animal pole and a tail bud vegetally (Fig. 1a). In contrast, in *boz din* mutants, most cells accumulated vegetally, creating a giant tailbud, whereas the head and trunk rudiments were absent. However, *boz din* mutants exhibited a residual dorso-ventral asymmetry in cell accumulation (Fig. 1b). During segmentation, when 10 somites were visible in wild-type siblings (Fig. 1c), the most severely affected *boz din* mutants had no somites (Fig 1d). At later stages (24 hpf), *boz din* mutants formed several somites encircling the yolk cell (Fig. 1h) that subsequently resided in the tail (Fig. 1i, 30 hpf).

If *boz* and *din* function redundantly in limiting BMP signaling, then the severe morphological defects in *boz din* mutants should be correlated with greatly increased *bmp* expression compared with either single mutant. During early gastrulation (6.5 hpf), *bmp4* is normally expressed ventrolaterally and in a discrete dorsal domain (Fig. 2a) (Nikaido et al. 1997). The dorsal domain was absent in *boz* and *boz din* mutants (data not shown, Fig. 2b). Consistent with the above hypothesis, the ventrolateral *bmp4* expression domain was more dorsally expanded in *boz din* mutants compared with either single mutant (Fig. 2b). Similarly, the ventrolateral marker *eve1* was more expanded in *boz din* mutants (Fig. 2c,d) than in either single mutant (data not shown) (Hammerschmidt et al. 1996; Fekany-Lee et al. 2000). Later, during segmentation, the tailbud *bmp4* expression domain was almost normal in *boz*, somewhat expanded in *din*, but dramatically expanded in *boz din* embryos (Fig. 2e–h; data not shown). Together, these morphological and gene expression analyses indicated that most cells in *boz din* mutants resided in the prospective tailbud region within a greatly expanded *bmp4* expression domain (cf. Figs. 1 and 2). Furthermore, *boz* and *din* function synergistically in negative regulation of *bmp4* expression.

The loss of head and trunk neural tissue in *boz din* mutants is likely a consequence of widespread *bmp* expression, because BMP signaling shifts cells from neural to epidermal/nonneural fates (Neave et al. 1997; Sasai and De Robertis 1997; Wilson et al. 1997). *gata3*, a marker of prospective nonneural ectoderm in wild-type-
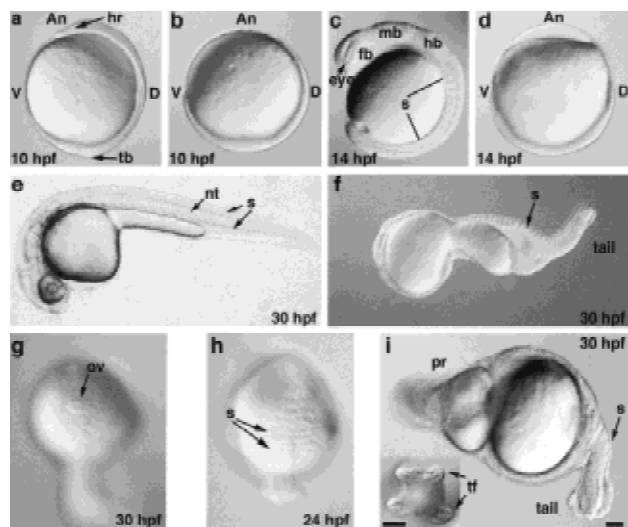

Figure 1. *boz din* mutant embryos fail to develop a head and trunk. Live (*a,c,e*) wild-type and (*b,d,f–i*) *boz din* mutant embryos at (*a,b*) 10 hpf, (*c,d*) 14 hpf, (*h*) 24 hpf, and (*e–g,i*) 30 hpf. (*g*) Single otic vesicle was often found as the most anterior structure in the less affected class of double *boz din* mutants. (*i*) Inset shows tail fin duplication. (*a–f,i*) Lateral views, dorsal to *right*; (*i*) dorsal views, anterior to *top*; (*g*) anterior view; (An) Animal; (D) dorsal; (V) ventral; (hr) head rudiment; (tb) tailbud; (fb) forebrain; (mb) midbrain; (hb) hindbrain; (nt) notochord; (ov) otic vesicle; (pr) protrusion; (s) somite; (tf) tail fin. Bar, 100 µm.
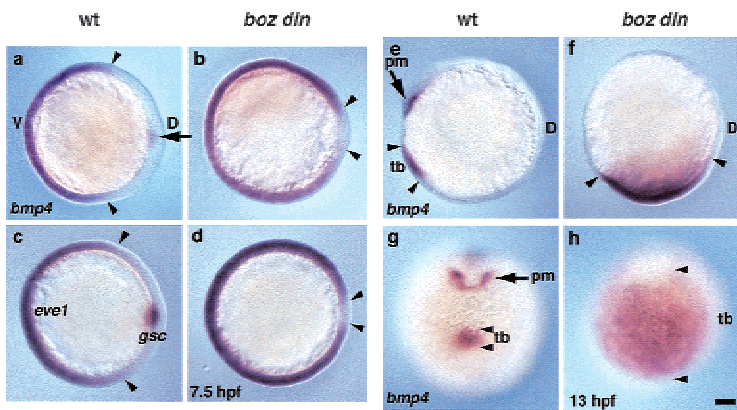
wt	*boz din*	wt	*boz din*

Figure 2. *bmp4* expression is greatly expanded in *boz din* mutants. *bmp4* expression in (*a*) wild-type (wt) and (*b*) *boz din* embryos at mid-gastrulation (7.5 hpf). Ventro-lateral *eve1* expression and organizer-specific expression of *gsc* was used to distinguish (*c*) wild-type and (*d*) *boz din* embryos at mid-gastrulation (7.5 hpf). *bmp4* expression in (*e,g*) wild-type and (*f,h*) *boz din* embryos during somitogenesis (13 hpf). (*a–d*) Anterior views, dorsal to *right*; (*e,f*) lateral views, dorsal to *right*; (*g,h*) ventral views. Arrowheads indicate borders of (*a–d*) ventro-lateral and (*e–h*) posterior domains of *bmp4* and *eve1* expression; arrow indicates (*a*) dorsal domain and (*e,g*) anterior *bmp4* expression domain absent in *boz din*. (pm) Prechordal mesoderm; (tb) tailbud. Bar, 100 μm.

late gastrulae (Fig. 3a), was moderately expanded in *boz* and *din* mutants (data not shown) (Neave et al. 1995; Fekany-Lee et al. 2000). In contrast, in *boz din* embryos, *gata3* expression spread dorsally, revealing a severe reduction of prospective neural ectoderm (Fig. 3b). *HuC* expression, marking neuronal precursors along the entire axis in wild-type embryos (Fig. 3c; Kim et al. 1996), was limited to a few putative tail neurons in *boz din* mutants (Fig. 3d). Furthermore, markers of the forebrain (*six3*), midbrain–hindbrain boundary (*pax2.1*), and hindbrain rhombomeres 3 and 5 (*krox20*) were absent in *boz din* mutants (Fig. 4e,f; Krauss et al. 1991; Oxtoby and Jowett 1993; Kobayashi et al. 1998). Therefore, *boz din* mutants display a dramatic reduction of head and trunk neuroectoderm, and a concomitant expansion of nonneural ectoderm.

To investigate the defects underlying the apparent loss of head and trunk mesoderm in *boz din* mutants (Fig. 1i), we analyzed early mesendoderm development. During gastrulation, the panmesodermal marker *no tail* (*ntl*) is expressed in marginal mesoderm and dorsally in notochord precursors (Schulte-Merker et al. 1994). Although presumptive notochordal *ntl* expression was missing, marginal *ntl* expression encircled *boz* and *boz din* mutants throughout gastrulation, as in wild type (data not shown) (Hammerschmidt et al. 1996a; Fekany et al. 1999). Furthermore, two *nodal*-related genes essential for mesoderm formation, *cyclops* and *squint* (Feldman et al. 1998; Rebagliati et al. 1998; Sampath et al. 1998), were expressed normally in the blastoderm margin of *boz din* mutant blastulae. *boz din* mutants also retained endodermal expression of *sox17* (data not shown) and *axial*, but the chordamesoderm expression in the last one was missing (Fig. 3e,f) (Alexander and Stainier 1999).

Hence, initial stages of mesendoderm formation are not affected in *boz din* mutants, in contrast to Nodal signaling-deficient embryos (Feldman et al. 1998).

To investigate subsequent steps of mesoderm development, we analyzed *ntl* expression during segmentation, normally detected in the differentiating notochord and in tailbud mesodermal precursors (Fig. 3g). The notochordal *ntl* expression domain was reduced in *din* and absent in *boz* and *boz din* mutants (Fig. 3g,h) (Hammerschmidt et al. 1996a; Fekany et al. 1999). However, the tailbud mesodermal expression domain was normal in *boz*, expanded in *din*, and dramatically enlarged in *boz din* mutants, consistent with the massive accumulation of cells in this region, as mentioned above (cf. Fig. 3h with Fig. lb; data not shown). Similarly, tailbud expression of the mesodermal marker *paraxial protocadherin* (*papc*) was expanded in *boz din* compared with single mutants (Fig. 4a,b; data not shown) (Yamamoto et al. 1998). Conversely, expression of somitic markers, including *papc* and *myoD* (Weinberg et al. 1996) was not observed during early somitogenesis in *boz din* mutants, in contrast to single mutants (Fig. 4b). At the 15-somite stage, *myoD* marked an equivalent number of somites in wild-type, *boz*, and *din* embryos, but their number and size were greatly reduced in *boz din* mutants (Fig. 3i,j; data not shown). Together these studies suggest that in *boz din* mutants, an excess of mesoderm is present in the tailbud region at the expense of trunk somitic mesoderm.

We next determined whether the loss of somitic mesoderm in *boz din* embryos can be attributed to a transformation into ventral mesoderm. Expression of *gata1*, which marks blood precursors (Fig. 3g; Detrich et al. 1995), was normal in *boz* and slightly increased in *din* mutants (Hammerschmidt et al. 1996a; data not shown). In *boz din* mutants, *gata1*-positive cells were distributed abnormally, forming a narrow stripe around the embryonic circumference. Their number, however, was not greater than in *din* alone (Fig. 3h).

To further investigate the character of vegetally accumulating mesoderm in *boz din* mutants, we analyzed *caudal* (*cad*) expression, a marker of ventro-posterior mesoderm and ectoderm (Fig. 3k; Joly et al. 1992). Although the *cad* expression domain was enlarged in *din* mutants (data not shown), it was severely expanded toward the animal pole in *boz din* mutants such that most of the cells present in the embryo expressed *cad* (cf. Fig. 3l to Fig. 1b). Together these studies indicate that, whereas mesoderm is induced normally around the blastoderm margin of *boz din* mutants, during later development it accumulates vegetally and is misspecified toward a posterior character.

To investigate whether locally increased cell death contributed to the loss of dorso-anterior tissues in *boz din* mutants, we performed TUNEL analysis (Abdelilah et al. 1996). The number of apoptotic cells at 12 somites in *boz* mutants was similar to wild type (Fig. 3m; data
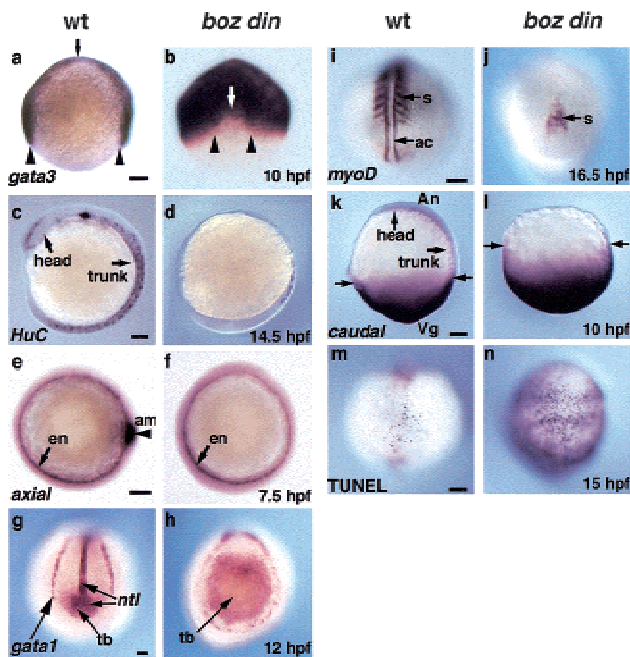
Figure 3. *boz din* mutants exhibit reduced neuroectoderm and dorsal mesoderm and expanded nonneural ectoderm and ventroposterior tissues. *gata3* expression in nonneural ectoderm in (*a*) wild type (wt) and (*b*) *boz din* mutants at 10 hpf. Arrowheads indicate width of the neural plate, arrows indicate anterior border of the neural plate. Neuronal *HuC* expression in (*c*) wild type and (*d*) *boz din* at 14.5 hpf. *axial* expression in endoderm and axial mesoderm (*e*) wild type and (*f*) *boz din* mutants at 7.5 hpf. *ntl* and *gata1* expression in (*g*) wild type and (*h*) *boz din* at 12 hpf. *myoD* expression in (*i*) wild type and (*j*) *boz din* at 15 somites (16.5 hpf). *cad* expression in (*k*) wild type and (*l*) *boz din* at 10 hpf. Arrows denote posterior border of *cad* expression. Cell death visualized by TUNEL staining in (*m*) wild type and (*n*) *boz din* at 15 hpf. (*a,b*) Animal view, dorsal to *left* (*a*); (*c,d,i,j*) dorsal views, anterior to *top*; (*e,f,k,l*) lateral views, anterior to *top*; (*g,h,m,n*) dorso-posterior views, anterior to *top*; (am) axial mesoderm; (en) endoderm; (s) somites; (ac) adaxial cells; (tb), tailbud. Bar, 100 µm.

not shown), increased posteriorly in *din* mutants (Hammerschmidt et al. 1996a), but greatly increased throughout *boz din* mutants (Fig. 3n). Whereas the increase in cell death in all regions of *boz din* mutants may contribute to a global tissue loss, it cannot account for the specific deficiency of head and trunk.

Next we asked whether the synergistic loss of head and trunk in *boz din* mutants is solely the result of excess BMP activity or redundant, BMP-independent functions of *boz* and *din*. To address this issue, we used the *swirl^{tc300}* (*swr*) mutation, which inactivates the *bmp2b* locus and leads to down-regulation of *bmp4* and *bmp7* and consequently to a dorsalized phenotype (Kishimoto et al. 1997; Nguyen et al. 1998; Schmid et al. 2000). First, we examined phenotypes of *din;swr* and *boz;swr* double mutants. Double *din;swr* mutants and *swr* single mutants exhibit an identical dorsalized phenotype, consistent with *din* acting exclusively in a BMP-dependent manner (Hammerschmidt et al. 1996b). In contrast, in

boz;swr mutants, the neural induction deficit of *boz* was suppressed, but not the notochord or forebrain deficiencies. The uninterrupted circumferential expression of the presomitic mesodermal marker *papc* indicated that ventrolateral mesoderm was dorsalized as in *swr* mutants and that the notochord was absent as in *boz* mutants (Fig. 4d). Further, reduced *six3* expression in the forebrain, a hallmark of the *boz* phenotype (Fekany-Lee et al. 2000), was also observed in *boz;swr* mutants (Fig. 4h). However, markers of the midbrain–hindbrain boundary (*pax2.1*) and hindbrain (*krox20*) encircled the embryo in *boz;swr* mutants (Fig. 4h), as observed for *swr* mutants (Fig. 4g). These observations are consistent with the results of inhibiting BMP signaling in *boz* mutants by overexpressing Chordin or Noggin, and genetically confirm that the notochord and forebrain deficiencies in *boz* are caused by a BMP-independent defect (Fekany-Lee et al. 2000). Finally, we analyzed the *boz din;swr* triple mutants. Because *swr* is epistatic to *din* (Hammerschmidt et al. 1996b), if the synergistic loss of head and trunk in *boz din* mutants is due solely to excess BMP activity, the *boz din;swr* triple and *boz;swr* double-mutant phenotypes should be identical. *boz din;swr* triple mutants exhibited circumferential *papc* expression, indicating that the ventral mesoderm was dorsalized, and the notochord was still absent (Fig. 4d), just like *boz;swr*. In addition, the ectoderm was completely neuralized, but the forebrain was still reduced (Fig. 4h). These epistatic analyses demonstrate that the synergistic loss of head and trunk in *boz din* mutants is due to excessive BMP signaling. Hence, *boz* and *din* have redundant functions in inhibition of BMP activity during head and trunk development.

For the first time, our studies show that simultaneous inactivation of the zygotic functions of only two genes, *boz* and *din*, can result in embryos without a head and trunk. To date, this dramatic phenotype has only been generated by embryological manipulations such as early removal of dorsal determinants or high-level BMP overexpression (Scharf and Gerhart 1983; Clement et al. 1995; Jesuthasan and Strahle 1997; Kishimoto et al. 1997; Neave et al. 1997; Ober and Schulte-Merker 1999). As removal of dorsal determinants from vegetal pole of zebrafish zygote results in loss of *boz* and *din* expression (Ober and Schulte-Merker 1999), we hypothesize that these two genes identify the two main pathways activated by dorsal determinants to limit BMP signaling during head and trunk development. Although *boz din* mutants have severe axis truncations, they still exhibit some dorsal-ventral polarity at the gastrula stage, and form a rudimentary tail (Figs. 1b,i and 2a,b). Therefore, *boz din* may not completely remove anti-BMP functions, raising the possibility that another BMP antagonist(s) is residually active in these mutant embryos.

The findings described here show that several distinct effects of high BMP activity cause the head/trunk deficiency in *boz din* double mutants. Within the ectoderm, high levels of BMP activity transform the neuroectoderm into nonneural ectoderm, consistent with previous reports (Neave et al. 1997; Sasai and De Robertis 1997;
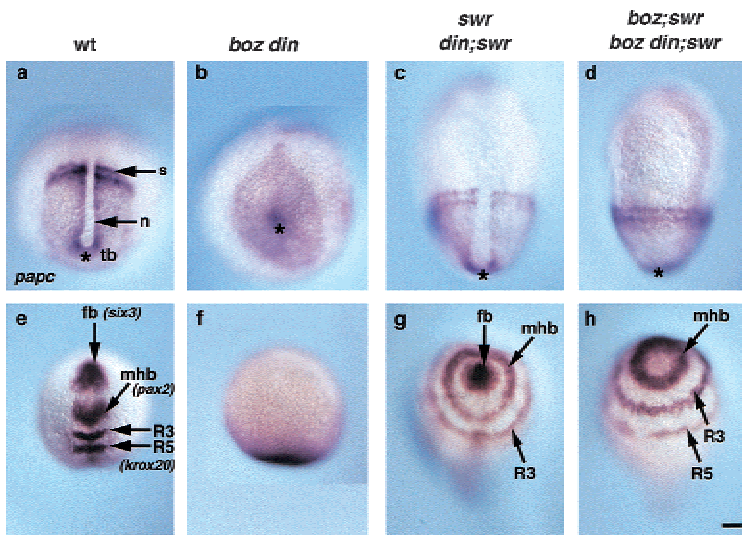
Figure 4. The synergistic defects of *boz din* mutants are suppressed in *boz din;swr* (*bmp2b*) mutants. Because *swr* is epistatic to *din* (Hammerschmidt et al. 1996b), the phenotype of *swr* and *din;swr* and likewise of *boz;swr* and *boz din;swr* were identical. *papc* expression in (*a*) wild type, (*b*) *boz din*, (*c*) *swr* (or *din;swr*), and (*d*) *boz din;swr* (or *boz;swr*) at 2–4 somites. (*) Position of the tailbud. *six3* (fb), *pax2.1* (mhb), and *krox20* (R3 and R5) expression in (*e*) wild type, (*f*) *boz din*, (*g*) *swr* (or *din;swr*), and (*h*) *boz din;swr* (or *boz;swr*). (*a–d*), Dorsal views, anterior to *top*; (*e–h*), dorso-anterior views; (s), somites; (n) notochord; (tb) tailbud; (fb) forebrain; (mhb) midbrain-hindbrain boundary; (R3) rhombomere 3; (R5) rhombomere 5. Bar, 100 µm.

Wilson et al. 1997). Our data suggest that almost all of the mesodermal precursors in *boz din* mutants experience very high levels of BMP activity and, instead of contributing to head and trunk, are misallocated to the tailbud, express ventro-posterior markers, and form a tail. This idea is in accord with fate-mapping studies showing that ventral cells in the zebrafish gastrula migrate to the tailbud and contribute to the tail (Kimmel et al. 1990; Kanki and Ho 1997), and this behavior is expanded dorsally in mutants with elevated BMP activity (D. Myers and L. Solnica-Krezel, unpubl.). Therefore, we propose that the high levels of BMP signaling in *boz din*
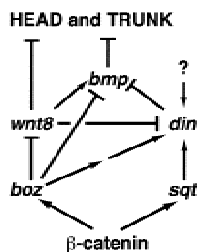

Figure 5. *boz* and *din* act in redundant, partially overlapping pathways to inhibit BMP function and specify head and trunk formation. Inactivation of *boz* leads to BMP-independent defects due to excess of Wnt (most likely Wnt8) signaling. Expression of *din* during late gastrulation is regulated by *boz* and *sqt*-independent mechanism (marked by ?), as *boz;sqt* double mutants are less ventralized than *boz din* double mutants (Hammerschmidt et al. 1996a; Fekany-Lee et al. 2000; Shimizu et al. 2000; Sirotkin et al. 2000).

embryos specify posterior structures at the expense of anterior structures. This proposal is consistent with the phenotype of BMP signaling mouse mutants, in which the major defect arises in posterior structures, such as the tail and allantois (Winnier et al. 1995). In summary, *boz* and *din* represent the major overlapping pathways (Fig. 5) that are absolutely essential to limit BMP activity dorso laterally and allow head and trunk formation in the vertebrate embryo.

Materials and methods

Fish strains
For all studies performed here, we used the *m168* allele of *boz* encoding a truncated protein without a homeodomain (Fekany et al. 1999). *m168* is considered to be a strong allele, however, low amounts of wild-type activity have been reported for this allele (Koos and Ho 1999). The *tt250* allele of *din* was used, encoding a truncated protein that lacks all the cysteine-rich repeats (Schulte-Merker et al. 1997). The *tc300* allele of *swr* was used, in which a tryptophan is substituted for one of the conserved cysteine residues (Kishimoto et al. 1997).

Genotyping
Live embryos were genotyped by PCR using a restriction polymorphism introduced by ENU mutations. Single live embryos at 10–24 hpf were digested in 2.8 mg/mL Proteinase K overnight at 65°C. After boiling for 10 min, 2 µL of digested solution served as a template in a 10-µL PCR reaction. *boz;swr* embryos showed a variable phenotype, similar to *boz* single mutants and occurred at an average frequency of 1.4% (*n* = 1085). *boz din;swr* embryos exhibited a more stable phenotype and the combination of *boz;swr* and *boz din;swr* embryos observed was 2.4% (*n* = 1609).

References

Abdelilah, S., Mountcastle-Shah, E., Harvey, M., Solnica-Krezel, L., Schier, A.F., Stemple, D.L., Malicki, J., Neuhauss, S.C.F., Zwartkruis, F., Stainier, D.Y.R., et al. 1996. Mutations affecting neural survival in zebrafish. *Development* **123:** 217–227.

Alexander, J. and Stainier, D.Y. 1999. A molecular pathway leading to endoderm formation in zebrafish. *Curr. Biol.* **9:** 1147–1157.

Bachiller, D., Klingensmith, J., Kemp, C,. Belo, J.A., Anderson, R.M., May, S.R., McMahon, J.A., McMahon, A.P., Harland, R.M., Rossant, J., et al. 2000. The organizer factors Chordin and Noggin are required for mouse forebrain development. *Nature* **403:** 658–661.

Brannon, M. and Kimelmann, D. 1996. Activation of *Siamois* by the Wnt Pathway. *Dev. Biol.* **180:** 344–347.

Clement, J.H., Fettes, P., Knochel, S., Lef, J., and Knochel, W. 1995. Bone morphogenetic protein 2 in the early development of *Xenopus laevis*. *Mech. Dev.* **52:** 357–370.

Detrich III, H.W., Kieran, M.W., Chan, F.Y,. Barone, L.M., Yee, K., Rundstadler, J.A., Pratt, S., Ransom, D., and Zon, L.I. 1995. Intraembryonic

hematopoietic cell migration during vertebrate development. *Proc. Natl. Acad. Sci.* **92:** 10713–10717.

Fekany, K., Yamanaka, Y., Leung, T., Sirotkin, H.I., Topczewski, J., Gates, M.A., Hibi, M., Renucci, A., Stemple, D., Radbill, A., et al. 1999. The zebrafish *bozozok* locus encodes Dharma, a homeodomain protein essential for induction of gastrula organizer and dorsoanterior embryonic structures. *Development* **126:** 1427–1438.

Fekany-Lee, K., Gonzalez, E., Miller-Bertoglio, V., and Solnica-Krezel, L. 2000. The homeobox gene *bozozok* promotes anterior neuroectoderm formation in zebrafish through negative regulation of BMP24 and Wnt pathways. *Development* **127:** 2333–2345.

Feldman, B., Gates, M.A., Egan, E.S., Dougan, S.T., Rennebeck, G., Sirotkin, H.I., Schier, A.F., and. Talbot, W.S. 1998. Zebrafish organizer development and germ-layer formation require nodal-related signals. *Nature* **395:** 181–185.

Hammerschmidt, M., Pelegri, F., Mullins, M.C., Kane, D.A., van Eeden, F.J.M., Granato, M. Brand, M., Furutani-Seiki, M., Hafter, P., Heisenberg, C.-P., et al. 1996a. *dino* and *mercedes*, two genes regulating dorsal development in the zebrafish embryo. *Development* **123:** 95–102.

Hammerschmidt, M., Serbedzija, G.N., and McMahon, A. 1996b. Genetic analysis of dorsoventral pattern formation in the zebrafish: Requirement of BMP-like ventralizing activity and its dorsal repressor. *Genes* & *Dev.* **10:** 2452–2461.

Jesuthasan, S. and Strahle, U. 1997. Dynamic microtubules and specification of the zebrafish embryonic axis. *Curr. Biol.* **7:** 31–42.

Joly, J.S., Maury, M., Joly, C., Duprey, P., Boulekbache, H., and Condamine, H. 1992. Expression of a zebrafish caudal homeobox gene correlates with the establishment of posterior cell lineages at gastrulation. *Differentiation* **50:** 75–87.

Kanki, J.P. and Ho, R.K. 1997. The development of the posterior body in zebrafish. *Development* **124:** 881–893.

Kim, C.H., Ueshima, E., Muraoka, O., Tanaka, H., Yeo, S.Y., Huh, T.L., and Miki, N. 1996. Zebrafish elavHuC homologue as a very early neuronal marker. *Neurosci. Lett.* **216:** 109–112.

Kimmel, C.B., Warga, R.M., and Schilling, T.F. 1990. Origin and organization of the zebrafish fate map. *Development* **108:** 581–594.

Kishimoto, Y., Lee, K.H., Zon, L., Hammerschmidt, M., and Schulte-Merker, S. 1997. The molecular nature of zebrafish swirl: BMP2 function is essential during early dorsoventral patterning. *Development* **124:** 4457–4466.

Kobayashi, M., Toyama, R., Takeda, H., Dawid, I.B., and Kawakami, K. 1998. Overexpression of the forebrain-specific homeobox gene *six3* induces rostral forebrain enlargement in zebrafish. *Development* **125:** 2973–2982.

Koos, D.S. and Ho, R.K. 1999. The nieuwkoiddharma homeobox gene is essential for bmp2b repression in the zebrafish pregastrula. *Dev. Biol.* **215:** 190–207.

Krauss, S., Johansen, T., Korzh, V., and Fjose, A. 1991. Expression of the zebrafish paired box gene pax[zf-b] during early neurogenesis. *Development* **113:** 1193–1206.

Laurent, M.N., Blitz, I.L., Hashimoto, C., Rothbacher, U., and Cho, K.W. 1997. The *Xenopus* homeobox gene twin mediates Wnt induction of goosecoid in establishment of Spemann's organizer. *Development* **124:** 4905–4916.

Miller-Bertoglio, V., Carmany-Rampey, A., Furthauer, M., Gonzalez, E., Thisse, C., Thisse, B., Halpern, M.E., and Solnica-Krezel, L. 1999. Maternal and zygotic activity of the zebrafish ogon locus antagonizes BMP signaling. *Dev. Biol.* **214:** 72–86.

Mizuno, T., Yamaha, E., Kuroiwa, A., and Takeda, H. 1999. Removal of vegetal yolk causes dorsal deficencies and impairs dorsal-inducing ability of the yolk cell in zebrafish. *Mech. Dev.* **81:** 35–47.

Neave, B., Rodway, A., Wilson, S.W., Patient, R., and Holder, N. 1995. Expression of zebrafish GATA3 (gta3) during gastrulation and neurulation suggests a role in the specification of cell fate. *Mech. Dev.* **51:** 169–182.

Neave, B., Holder, N., and Patient, R. 1997. A graded response to BMP-4 spatially coordinates patterning of the mesoderm and ectoderm in the zebrafish. *Mech. Dev.* **62:** 183–195.

Nguyen, V.H., Schmid, B., Trout, J., Connors, S.A., Ekker, M., and Mullins, M.C. 1998. Ventral and lateral regions of the zebrafish gastrula, including the neural crest progenitors, are established by a *bmp2bswirl* pathway of genes. *Dev. Biol.* **199:** 93–110.

Nikaido, M., Tada, M., Saji, T., and Ueno, N. 1997. Conservation of BMP signaling in zebrafish mesoderm patterning. *Mech. Dev.* **61:** 75–88.

Nikaido, M., Tada, M., Takeda, H., Kuroiwa, A., and Ueno, N. 1999. In vivo analysis using variants of zebrafish BMPR-IA: Range of action and involvement of BMP in ectoderm patterning. *Development* **126:** 181–190.

Ober, E.A. and Schulte-Merker, S. 1999. Signals from the yolk cell induce mesoderm, neuroectoderm, the trunk organizer, and the notochord in zebrafish. *Dev. Biol.* **167:** 167–181.

Oxtoby, E. and Jowett, T. 1993. Cloning of the zebrafish krox-20 gene (krx-20) and its expression during hindbrain development. *Nucleic Acids Res.* **210:** 1087–1095.

Rebagliati, M.R., Toyama, R., Haffter, P., and Dawid, I.B. 1998. *cyclops* encodes a nodal-related factor involved in midline signaling. *Proc. Natl. Acad. Sci.* **95:** 9932–9937.

Sampath, K., Rubinstein, A.L., Cheng, A.M.S., Liang, J.O., Fekany, K., Solnica-Krezel, L., Korzh, V., Halpern, M.E., and. Wright, C.V.E. 1998. Induction of the zebrafish ventral brain and floor plate requires CyclopsNodal Signaling. *Nature* **395:** 185–189.

Sasai, Y. and De Robertis, E.M. 1997. Ectodermal patterning in vertebrate embryos. *Dev. Biol.* **182:** 5–20.

Sasai, Y., Lu, B., Steinbeisser, H., and De Robertis, E.M. 1995. Regulation of neural induction by the chordin and Bmp-4 antagonistic patterning signals in Xenopus. *Nature* **376:** 333–337.

Scharf, S.R. and Gerhart, J.C. 1983. Axis determination in eggs of *Xenopus laevis*: A critical period before first cleavage, identified by the common effects of cold, pressure and ultraviolet irradiation. *Dev. Biol.* **99:** 75–87.

Schmid, B., Furthauer, M., Connors, S.A., Trout, J., Thisse, B., Thisse, C., and Mullins, M.C. 2000. Equivalent genetic roles for bmp7snailhouse and bmp2bswirl in dorsoventral pattern formation. *Development* **127:** 957–967.

Schneider, S., Steinbesser, H., Warga, R.M., and Hausen, P. 1996. β-catenin translocation into nuclei demarcates the dorsalizing centers in frog and fish embryos. *Mech. Dev.* **57:** 191–198.

Schulte-Merker, S., VanEeden, F.J.M., Halpern, M.E., Kimmel, C.B., and Nusslein-Volhard, C. 1994. No tail (Ntl) is the zebrafish homologue of the mouse T (brachyury) gene. *Development* **120:** 1009–1015.

Schulte-Merker, S., Lee, K.J., McMahon, A.P., and Hammerschmidt, M. 1997. The zebrafish organizer requires *chordino*. *Nature* **387:** 862–863.

Shimizu, T., Yamanaka, Y., Ryu, S., Hashimoto, H., Yabe, T., Hirata, T., Bae, Y., Hibi, M., and Hirano, T. 2000. Cooperative roles of Bozozok-Dharma and Nodal-related proteins in the formation of the dorsal organizer in zebrafish. *Mech. Dev.* **91:** 293–303.

Sirotkin, H.I., Dougan, S.T., Schier, A.F., and Talbot, W.S. 2000. bozozok and squint act in parallel to specify dorsal mesoderm and anterior neuroectoderm in zebrafish . *Development* **127:** 2583–2592.

Smith, W. and Harland, R. 1992. Expression cloning of noggin, a new dorsalizing factor localized to the Spemann organizer in *Xenopus* embryos. *Cell* **70:** 829–840.

Thisse, C. and Thisse, B. 1998. High resolution whole-mount *in situ* hybridization. *Zebrafish science monitor* **5:** 8–9.

Weinberg, E.S., Allende, M.L., Kelly, C.S., Abdelhamid, A., Murakami, T., Andermann, P., Doerre, O.G., Grunwald, D.J., and Riggleman, B. 1996. Developmental regulation of zebrafish MyoD in wild-type, no tail and spadetail embryos. *Development* **122:** 271–280.

Wilson, P.A. and Hemmati-Brivanlou, A. 1995. Induction of epidermis and inhibition of neural fate by Bmp-4. *Nature* **376:** 331–333.

Wilson, P.A., Lagna, G., Suzuki, A., and Hemmati-Brivanlou, A. 1997. Concentration-dependent patterning of the *Xenopus* ectoderm by BMP4 and its signal transducer Smad1. *Development* **124:** 3177–3184.

Winnier, G., Blessing, M., Labosky, P.A., and Hogan, B.L. 1995. Bone morphogenetic protein-4 is required for mesoderm formation and patterning in the mouse. *Genes* & *Dev.* **9:** 2105–2116.

Yamamoto, A., Amacher, S.L., Kim, S.H., Geissert, D., Kimmel, C.B., and De Robertis, E.M. 1998. Zebrafish *paraxial protocadherin* is a downstream target of spadetail involved in morphogenesis of gastrula mesoderm. *Development* **125:** 3389–3397.